Laser and Particle Beams (2007), *25*, 489–495. Printed in the USA.

DOI: 10.1017/S0263034607000602

Plasma diagnostics by means of the scattering of electrons and proton beams

E. NARDI,[1] Y. MARON,[1] AND D.H.H. HOFFMANN[2]
[1]Faculty of Physics, Weizmann Institute of Science, Rehovoth Israel
[2]GSI-Darmstadt and Institut für Kernphysik, Technische Universität Darmstadt, Darmstadt, Germany

(Received 1 March 2007; Accepted 23 May 2007)

Abstract

Scattering of energetic electron and proton beams by cold matter is significantly different from the scattering of these particles by plasma, which may be either highly ionized or dense strongly coupled plasma. This is due to the difference in the shielding of the target nuclei between the two cases. Quantitatively, we treat the problem by means of the Bethe Moliere multiple scattering theory and the version of this theory for plasma as derived by Lampe. We propose to use this effect as a plasma diagnostic tool, utilizing monoenergetic, well-collimated electron or proton beams produced either by femtosecond laser plasma interactions or by accelerators. The effect is first illustrated for simplicity, by calculating the widths of the angular distribution of scattered particles interacting with the extreme cases of very hot fully ionized carbon, and iron plasmas, and comparing these results to the corresponding cold material. The more relevant case of electron scattering from partially ionized iron and carbon plasmas covering the entire range from a cold to a completely ionized target is also dealt with here. This paper brings up and highlights the difference between scattering by plasma and by cold material in light of the recent proposals to employ particle beams for various fusion applications.

Keywords: Electron beams; Fully ionized plasma; Partially ionized plasma; Proton beams; Scattering

1. INTRODUCTION

In this paper, we deal with the difference in the scattering of energetic electrons and protons interacting with plasma as opposed to scattering from cold targets. The difference in the width of the distribution of the scattered particles increases with the degree of target ionization and is dependent on the plasma properties. In this connection, we propose using intense, well collimated, monoenergetic electron and proton beams, for probing and diagnosing high Z plasma targets. Such well defined beams could be extracted either from intense femtosecond laser target interactions (Flippo *et al.*, 2007; Koyama *et al.*, 2006; Lifshitz *et al.*, 2006; Yin *et al.*, 2006; Glinec *et al.*, 2005) or from an accelerator. The basis of the proposal is the measurement of the angular distribution of the exiting beam particles from the probed plasma column. We also note that the topic brought up here should also be of significance in connection with particle beam assisted fusion (Deutsch *et al.*, 1996, Someya *et al.*, 2006) as well as for diagnostics employing particle beams (Wetzler *et al.*, 1997; Mackinnon *et al.*, 2004).

Address correspondence and reprint requests to: Eran Nardi, Faculty of Physics, Weizmann Institute of Science, Rehovoth 76100, Israel. E-mail: eran.nardi@weizmann.ac.il

Multiple scattering of particle beams is predominately due to their Coulomb interaction with the target nuclei. The shielding of this interaction by the target electrons, which is detrimental to the amount of scattering, depends on the state of the target. We first illustrate this for simplicity by comparing two extremes for the specific cases of carbon and iron; the first extreme is a cold target and the second is a fully ionized plasma target. The screening length for a Yukawa type potential is taken as the distance where the potential a drops to the value of $1/e$ as compared to the potential at the origin. The screening length for a cold target is about the atomic dimensions (Moliere, 1948; Bethe, 1953). In the completely ionized plasma target of density significantly smaller than solid density, the much longer Debye radius (Lampe, 1970) screens the Coulomb potential of the target nucleus. The screening length is now given by this quantity as compared to the cold atom where it is about the atomic dimension. The shielding is thus less effective in the completely ionized plasma and the angular dispersion of the scattered beam larger. For partially ionized plasma, the situation is more complex, and the amount of scattering here is intermediate between the cold and fully ionized target. In Section 2, the theory for the cold, fully ionized, as well as for the partially ionized

plasma are given. The theoretical treatment for the three regimes is based on the Moliere-Bethe theory of multiple scattering (Moliere, 1948; Bethe, 1953) and has been addressed previously for high Z plasma (Nardi & Zinamon, 1978) In Section 3, we present results of scattering from fully ionized iron and carbon targets, for monoenergetic electron, and proton beams. Partially ionized plasma results are also given for iron and carbon targets for 5 MeV relativistic electron beams, covering the range from a cold to a completely ionized target. In Section 4, we conclude and discuss the results.

2. THEORY

2.1. Fully ionized plasma and cold target

Scattering from cold and fully ionized targets is treated here by means of the Moliere-Bethe theory of multiple scattering (Moliere, 1948; Bethe, 1953). This theory is amenable for quantitatively treating each of the different targets by means of the appropriate screening length for the given target. The effect of the screening length on particle scattering is discussed above in a qualitative manner and will now be presented in a quantitatively.

The angular distribution of charged particles is essentially dependent, according to this theory, on a single parameter (excluding the thickness and atomic number of the target), the screening angle χ_α, which is based on the angle χ_0, given by, $\chi_0 = (\hbar/\mathrm{p})/a_{scr}$ the de-Broglie wavelength divided by the screening length (Bethe, 1953). The screening length a_{scr}, of the target nucleus by the bound electrons in the cold target can be well approximated by the Thomas-Fermi screening length given by, $0.885a_0\mathrm{Z}^{-1/3}$, where a_0 is the Bohr radius and Z is the atomic number of the target (Moliere, 1948; Bethe, 1953).

In his derivation for cold material, Moliere (1948) multiplies χ_0, by the factor $(1.13 + 3.76\alpha^2)^{1/2}$, where α is the usual parameter $z\mathrm{Ze}^2/\hbar v$, with z being the atomic number of the projectile. Bethe (1953) attributes this factor to deviation from the first Born approximation. Some inconsistencies exist in these and other approximations introduced by Moliere (Nigam *et al.*, 1959), but calculations using the Moliere procedure agree well enough with experimental results for both protons and electrons. Moliere's final result for the screening angle, χ_α in cold material is

$$\chi_\alpha = \chi_0 \cdot (1.13 + 3.76\alpha^2)^{1/2}. \quad (1)$$

In the completely ionized plasma, the screening length, a_{scr}, was shown by Lampe (1970), to be the Debye length, which accounts for shielding due to both the free electrons and plasma ions and which is given by: $D = [kT/(4\ \pi\ n_e(\mathrm{Z}+1)\mathrm{e}^2)]^{1/2}$, where Z is the atomic number of the target, and $\mathrm{n_e}$ is the free electron density. In his derivation of the Bethe Moliere theory for plasma, Lampe (1970) included dynamical screening which he introduced by means of the quantum Lenard Balescu equation, see Eq. (4) below. For the screening angle of the plasma he thus obtained, $\chi_{\mathrm{pl}} = (\hbar/p)/D$

In order to calculate the width of exiting scattered beam, the two quantities χ_c and B defined in the Bethe-Moliere theory are needed. The former is an angle indicative of the thickness L of the slab and of the atomic number Z and where N is the number of scattering atoms per cm^3, it is given by,

$$\chi_c^2 = 4\pi\mathrm{Ne}^4 LZ(1+Z)/(pv)^2. \quad (2)$$

The effect of inelastic electron scattering is introduced by replacing Z^2 with $Z(Z+1)$. Fano (1954) has however shown that this is correct for electrons with an additional small correction in Eq. (3) below, but not for protons. For the cases studied here, the Fano corrections have essentially no effect on the results.

B is obtained by solving the following equation for cold matter (Moliere, 1948; Bethe, 1953), where $\gamma = 0.5772$

$$B\text{-}\ln B = \ln(\chi_c/\chi_\alpha)^2 + 1 - 2\gamma. \quad (3)$$

For the completely ionized plasma (Lampe, 1970), B is obtained from,

$$B\text{-}\ln B = \ln(\chi_c/\chi_{\mathrm{pl}}) + 2 - 2\gamma. \quad (4)$$

Thus, by using the quantum Lenard-Balescu equation in order to account for dynamical screening, a small change of about unity appears in the equation for B, the parameter that determines the width of the angular distribution, compared to this equation for the case of cold matter. By assuming static Debye screening, Eq. (4) takes the form of Eq. (3), each equation with its appropriate screening lengths.

The width of the angular distribution, given here as the angle where the distribution assumes a value of $1/\mathrm{e}$ of its peak value at 0 degrees, is according to the Moliere-Bethe theory given by, $\chi_\mathrm{c}\mathrm{B}^{1/2}$.

Relativistic electrons or protons could each be employed in these types of studies. Electrons have the experimental advantage of being scattered to significantly larger angles at the same kinetic energies for the same target thicknesses. The interaction of intense electron beams with dense plasma targets could be complex with various instabilities coming into play (Bret *et al.*, 2007; Firpo *et al.*, 2006; Jung *et al.*, 2005). Such interaction would hamper the analysis although at lower beam intensities they could be negligible. An interesting aspect of the current proposal is the possibility to ascertain the appearance of the instabilities in the electron interaction, which clearly modify electron flow within the plasma. Proton interactions with dense plasma targets are free from such phenomena; however, the experiment must be designed such that the dynamic screening length of the swift protons

https://doi.org/10.1017/S0263034607000602 Published online by Cambridge University Press

given by v/ω_p, is significantly greater than the plasma Debye length. One could envisage conducting both types of experiments even complementing them with ion beams.

Energy loss of either proton or electron beams provide information regarding the mass of the target traversed by the beam which is needed in order to quantify the extent of angular dispersion. Energy loss must include plasma-stopping effects (Nardi & Zinamon, 1978; Hoffmann *et al.*, 1990; Barriga-Carrasco & Potekhin, 2006) in a self-consistent manner with results of the plasma state as inferred by the beam scattering experiment.

2.2. Partially ionized plasma

A more involved approach is needed for calculating scattering from partially ionized plasma, where the Coulomb potential is of a more complicated form. We treat this here within the framework of the Moliere-Bethe theory (Moliere, 1948; Bethe, 1953) in a manner similar to related previous work (Nardi & Zinamon, 1978). The potential is approximated here by the sum of two exponentially screened potentials, the first describing the screening of the nuclear charge of the target by the bound electrons, with the second accounting for the screening of the residual ionized target by the free electrons.

As a first step the ionization stage of the atoms in the plasma at the given density and temperature under consideration was determined by means of Thomas-Fermi theory using the procedure derived by Latter (1955). Good agreement between the ionization states thus calculated to those obtained by the Inferno model (Liberman, 1979) and also by the Saha equation was obtained for the cases in which comparisons were made. The Thomas-Fermi method also provides the potential near the nucleus and enables us to compare the screening of the nucleus by the bound electrons, as a function of the plasma properties.

In his general procedure for calculating the screening angle χ_α, Moliere defines $q(\chi)$, as the ratio of the scattering cross section of the atom to that of Rutherford scattering. Assuming a Yukawa type potential, $V(r) = Z/r\exp(-r/a_{src})$, $q(\chi)$ is given within the first order Born approximation, see Eq. (6.11) in Scott (1963) by

$$q(\chi) = \chi^4/(\chi^2 + [(\hbar/p)/a_{scr})]^2)^2. \quad (5)$$

Moliere also proposes this as a general simple functional form; see Eq. (6.63) in Scott. The screening angle χ_α is calculated by introducing $q(\chi)$ into the following formula, see also Bethe (1953),

$$-\ln(\chi_\alpha) = \lim_{k\to\infty}\left[\int_0^k q(\chi)d\chi/\chi + 1/2 - \ln k\right]. \quad (6)$$

For the simple case of the exponentially screened potential, Moliere calculates the screening angle χ_α using the above equation such that it is equal exactly to $(\hbar/p)/a_{scr}$ in accordance with the discussion above. We follow this procedure for the more complex case of partially ionized plasma, where the potential around the isolated ion $V(r)$, is assumed for simplicity to be given by the sum of two exponentially screened potentials,

$$V(r) = Z_b\,exp(-r/a_{TF})/r + (Z - Z_b)\,exp(-r/D)/r, \quad (7)$$

where Z_b is the number of bound electrons out of the total number Z, a_{TF} is the exponential Thomas-Fermi screening length due to the bound electrons, and D is the Debye length of the plasma see above. As $r \to 0$, $V(r) = Z/r$, while for the totally ionized plasma and cold atom limits the potential assumed the correct form. Thus, for the sum of the two exponentially screened potentials and within the first Born approximation:

$$q(\chi) = \chi^4\{(Z_b/Z)/(\chi^2 + \chi_{TF}^2)^2 + ((Z - Z_b)/Z)/(\chi^2 + \chi_D^2)^2\}. \quad (8)$$

Inserting this into Eq. (6), we obtain for the screening angle of the partially ionized plasma, where $\chi_{TF} = (\hbar/p)/a_{TF}$ and $\chi_D = (\hbar/p)/D$:

$$\chi_\alpha = (\hbar/p)\Big/\left[a_{TF}^{Zb/Z}D^{(Z-Zb)/Z}\right]. \quad (9)$$

Expressing the potential as a sum of exponentials was carried out by Moliere (Moliere, 1948) who approximated the atomic potential as a sum of three screened exponentials, and then used Eq. (6) to calculate the screening angle.

For the sake of consistency, we have solved Eq. (3), with χ_α as defined in Eq. (9), i.e., with the assumption of static shielding, throughout the complete range of temperature from the cold to completely ionized target. For the completely ionized Fe target, for the lower density plasma, the scattering angle according to Eq. (4) is 20.7 degrees, while by using Eq. (3) the angle is 20.2 degrees. The difference in the scattering angle between the cold and fully ionized targets is thus 7% between the static and dynamic screening assumptions; the same 7% is also obtained for carbon at the same density for the 5 MeV electrons.

3. RESULTS

3.1. Fully ionized plasma, electrons

In Tables 1 and 2, we first give some quantitative examples for the extreme cases of fully ionized carbon and iron probed by relativistic electrons at 2, 5, and 15 MeV. The calculations are performed for homogeneous plasma columns of different lengths and mass thicknesses. These range from 0.1 cm for the denser plasma up to the hypothetical case of 100 cm for the low-density plasma, while the plasma densities are 10^{19} and 10^{21} ions/cm^3. The example of the very long column was taken in order to afford comparison with

https://doi.org/10.1017/S0263034607000602 Published online by Cambridge University Press

Table 1. *Scattering of electrons from a completely ionized carbon target at two different densities and temperature combinations, each for two different thicknesses. Width denotes the 1/e scattering angle, L is mass the thickness of the target. Results are also given in bold for cold targets with the same mass thickness. The cold target width does not depend on target density*

ro(cm^{-3})	T(eV)	d(cm)	L(mg/cm^2)	Width(deg) 2 MeV	5 MeV	15 MeV
10^{19}	100	10	2.0	3.26	1.43	0.51
10^{21}	200	0.1	2.0	2.82	1.24	0.44
	0		2.0	**1.62**	**0.71**	**0.25**
10^{19}	100	100	20	11.0	4.86	1.71
10^{21}	200	1.0	20	9.80	4.29	1.51
			20	**6.65**	**2.92**	**1.03**

the denser plasma for the same amount of material traversed by the beams. For the results given in both tables, the energy loss of the particle beams within the plasma was small compared to the incoming projectile energies.

In Table 1, which presents the results for carbon, for each of the incident beam energies, two different target mass thicknesses were tested, while for each thickness, two completely ionized plasmas of carbon of different density and temperature were calculated. The ion densities of the completely ionized carbon plasma were 10^{19} and 10^{21} cm^{-3} in both cases, the temperatures in each case were chosen such that the target was completely ionized for the given density. For each mass thickness, the width of the angular distribution for cold material is also given. Table 2 gives similar results for iron at the same densities and for mass columns of different thicknesses.

The angular distribution widths given below are the values of $\chi_c B^{1/2}$ the 1/e width of the angular distribution. These values are clearly broader in the plasma cases compared to the cold material in accordance to the discussion above. The angular distributions for the higher temperature lower density plasmas are broader than the corresponding lower temperature higher density case due to the increase in the Debye length, indicating sensitivity to the plasma conditions. Electron angular distribution widths obtained here, for Be, Fe, and Au were in good agreement with the results given in the literature.

Table 2. *Scattering of electrons from a completely ionized iron target at two different density and temperature combinations, each for two different thicknesses. Width denotes the 1/e scattering angle; L is the mass thickness of the target. Results are also given in bold for cold targets with the same mass thickness. The cold target width does not depend on target density*

ro(cm^{-3})	T(eV)	d(cm)	L(mg/cm^2)	Width(deg) 2 MeV	5 MeV	15 MeV
10^{19}	900	10	9.3	14.0	6.16	2.17
10^{21}	1200	0.1	9.3	12.2	5.36	1.89
	0		9.3	**8.04**	**3.53**	**1.24**
10^{19}	900	100	93	47.0	20.7	7.3
10^{21}	1200	1.0	93	41.7	18.4	6.47
	0		93	**30.4**	**13.3**	**4.69**

The lower the energy of the electrons, the broader the angular distributions, (see Eqs. (2) and (3)), as are the differences in the scattering angle between the plasma and cold cases. This difference is thus relevant to the basic effect discussed in this paper. Measurement of this plasma-cold target scattering effect is feasible for the 2 and 5 MeV cases even for the least sensitive case, that of the thinner mass column at the higher density of carbon. For iron at the lower density thin target conditions, the scattering effect could be observed at 15 MeV and certainly at the lower energies. Thus in general, by recording the scattered particles on a "screen" placed at an appropriate distance from the target, and by conducting good resolution experiments; the essential experimental information can be extracted. We note that by lowering the electron beam energy, the collisional frequency increases relative to the instability growth rate (Lampe, 1970). The larger the collisional frequency relative to instability growth rate, the less probable that beam plasma instabilities dominate electron beam propagation.

3.2. Fully ionized plasma, protons

As is evident from the formulae presented above, proton scattering is significantly smaller than electron scattering. In both the cases of electrons and protons, we have compared the results of our calculations to the published experimental data in the literature (Hanson *et al.*, 1955; Kulchitsky & Latyshev, 1942; Vincour & Bem, 1978; Bichel, 1958). In Table 3, we present the scattering results for protons on fully ionized carbon for the same plasma conditions as the electron results, for the thinner carbon target only. The thicker mass targets were not included in the proton tables since the energy loss in most cases was too large. Lowering the beam kinetic energy, the dynamic screening length increases. However, for the cases studied here, it is still significantly larger than the Debye length. The differences in the scattering angles between the cold and plasma cases are small for the thin targets and probably could be

Table 3. *Scattering of protons on completely ionized carbon targets. Width is the 1/e angle; L is the thickness is that of target. Results are also given in bold for cold targets with the same mass thickness as the two plasma targets. The cold target width does not depend on target density*

ro(cm^{-3})	T(eV)	d(cm)	L(mg/cm^2)	Width(deg) 2 MeV	5 MeV	15 MeV
10^{19}	100	10	2.0	2.27	0.88	0.28
10^{21}	200	0.1	2.0	2.04	0.79	0.25
	0		2.0	**1.45**	**0.55**	**0.17**

https://doi.org/10.1017/S0263034607000602 Published online by Cambridge University Press

measured for the 2 MeV case. As expected, the scattering angles as well as the plasma effect are larger for iron as seen in Table 4, especially for the 2 MeV proton case. In the latter case, the Debye length is about twice the dynamic screening length. Assuming that $1/a_{scr}$ is now the root of the sum of squares of the reciprocals of the Debye length plus that of the dynamic screening length, the scattering angle decreases by only about 1%.

3.3. Partially ionized plasma

Scattering from partially ionized iron and carbon plasma were calculated for electrons at the energy of 5 MeV. Two different densities were chosen for each element, while the temperatures scanned the range from a zero temperature target up to the temperature corresponding to the fully ionized target for the given plasma density. The densities for both iron and carbon were those of Tables 1 and 2, 10^{19} and 10^{21} ions/cm^3. The target thicknesses were 93 mg/cm^2 for both iron densities, and 20 mg/cm^2 for both carbon densities. The corresponding column lengths are 100 cm for the lower density and 1 cm for the higher density for both elements. As noted above, the long plasma column for the low density was adopted in order to afford a direct comparison with the higher density data.

The width of the angular distribution was calculated based on Eq. (3), the static screening approximation for the value of B. The screening angle was determined from Eq. (9), the derivation of which is based on the first order Born approximation. This approximation is satisfactory here since the value of the parameter α, the square of which is a measure of the deviation from this approximation (Bethe, 1953) is equal here to 0.19 for iron and 0.04 for carbon calculated below. The Thomas-Fermi calculation enables observing the variation of the screening by the bound electrons as a function of the plasma temperature. The screening length decreases with ionization and the difference does not exceed 20%. By varying a_{TF}, the Thomas-Fermi screening length, in Eq. (9) by 20% for the high temperature plasma, we essentially observe no effect on the plasma scattering angle as given by Eq. (9).

The width of the angular distribution as a function of temperature for the two densities in iron is presented in Figure 1. As is observed in Tables 1 and 2, the lower density plasma gives larger scattering angles for the same temperature, resulting from the longer Debye length at this density. The basic shapes of both curves are similar. In the low temperature region, the curve rises steeply, especially for the low-density plasma, while leveling off at about 200 eV at both densities. The sensitivity of scattering angle to temperature is significantly larger in the perhaps more relevant lower temperature region. A similar calculation for the thinner plasma targets at both densities, with the width of 9.3 mg/cm, gives similar results. The differences in scattering between the cold and warm cases are about 35% of the corresponding cases plotted in Figure 1, enough to make the measurements feasible.

In a similar manner, we present in Figure 2, the scattering angle versus temperature for carbon plasma at the densities of 10^{19} and 10^{21} ions/cm^3. Once more, the results span the region from a cold target to a completely ionized target. The results of Figure 2 are qualitatively the same as those of Figure 1. The lower density results are significantly higher than those at the higher density, while in both cases the slope of the curve is much larger in the lower temperature region than for the high temperature plasma, which again shows a leveling off behavior.

Table 4. *Scattering of protons on completely ionized iron targets. Width is the 1/e angle; L is the thickness is that of target. Results are also given in bold for cold targets with the same mass thickness as the two plasma targets. The cold target width does not depend on target density*

				Width(deg)		
ro(cm^{-3})	T(eV)	d(cm)	L(mg/cm^2)	2 MeV	5 MeV	15 MeV
10^{19}	900	10	9.3	9.58	3.75	1.20
10^{21}	1200	0.1	9.3	8.66	3.37	1.08
	0		9.3	**6.10**	**2.28**	**0.74**

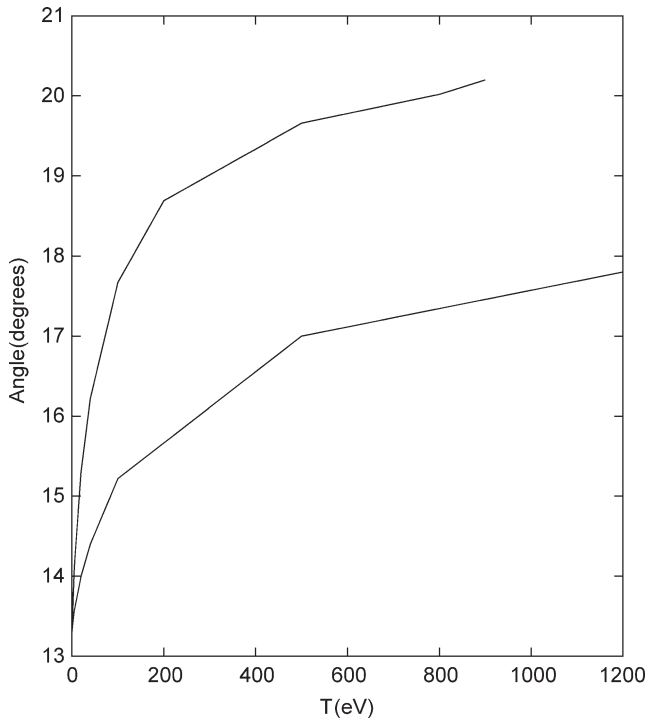

Fig. 1. Width of scattering distribution as a function of temperature for a collimated 5 MeV electron beam incident on a partially ionized iron plasma column, at two different plasma densities. The density of the top curve is 10^{19} while that of the bottom curve is 10^{21} ions/cm^3. The length of the higher density plasma column is 1 cm while that of the lower density plasma is 100 cm.

https://doi.org/10.1017/S0263034607000602 Published online by Cambridge University Press

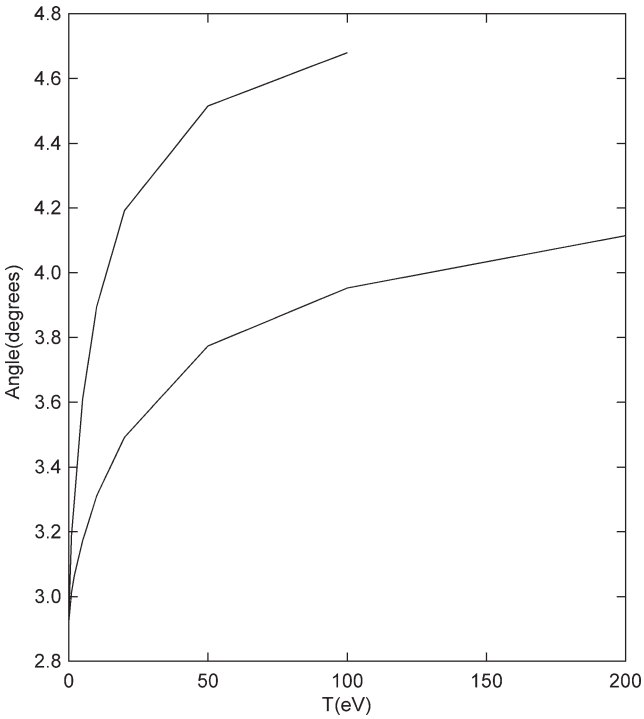

Fig. 2. Width of scattering distribution as a function of temperature for a collimated 5 MeV electron beam incident on a partially ionized carbon plasma column, at two different plasma densities. The density of the top curve is 10^{19} while that of the bottom curve is 10^{21} ions/cm^3. The length of the higher density plasma column is 1 cm while that of the lower density plasma is 100 cm.

4. DISCUSSION AND CONCLUSIONS

This paper deals with idealized homogeneous targets, where we have demonstrated for a variety of examples, the difference in scattering between plasma, both fully and partially ionized, compared to scattering from cold targets. For the practical cases of non-homogeneous targets, the approximation could be made whereby the target is divided into slabs of equal density and temperature. The thicknesses of these slabs must be sufficient such that the multiple scattering parameters B, defined in Eqs. (3) and (4) be at least about four. Scattering calculations could then be performed by means of the Monte Carlo method (Nardi & Zinamon 1978). In plasma targets of the type treated here, the values of B are much larger in these targets than for cold material, for an equivalent amount of mass traversed. This is due to the much longer screening length, see Eqs. (3) and (4). It is therefore possible to use this computational technique for thinner slabs compared to the cold material case. For example, for an iron plasma of 10^{21} ions/cm^3, for a thickness of 0.005 cm, the value of B is 10, while for cold material 20 times thicker we obtain $B = 5.7$. For targets in which the non-homogeneity is too large to employ the Moliere-Bethe method, the penetration of the beam particles must be treated by a detailed calculation of the scattering with each individual target atoms, or by other methods, (Barriga-Carrasco *et al.*, 2004). The above discussion highlights the possibility, pointed out above, of utilizing particle beam scattering as plasma diagnostic.

In the context of the work presented here, we should also like to comment on the scattering of electrons and protons in a DT core target, the situation encountered in the case of electron beam assisted fusion (Deutsch *et al.*, 1996), where the density is on the order of a 100 g/cm^3 with the temperature at about 5 keV. Since the plasma in these cases is weakly coupled, the screening is given by the Debye length, which at these conditions is about 0.710^{-8} cm, which is very close to the screening length of cold hydrogen, which is about half an Angstrom. Thus, the screening and therefore multiple scattering within the DT core is well approximated by assuming cold material in the core.

It is also worth noting that the influence of the plasma environment on scattering as discussed here could be of importance in proton radiography work (Mackinnon *et al.*, 2004), where accurate angular distribution data is measured and compared to theoretical analysis. It is of importance to stress here that the present communication also raises once more the effect of the plasma environment on the scattering of energetic particles in plasma as opposed to cold material.

In summary, we have shown the sensitivity of the scattering of electrons and protons to plasma target conditions, stressing the electrons, which give a larger effect. Calculations were carried out for fully ionized as well as partially ionized Fe and C targets, each at two different densities. The Moliere-Bethe theory of multiple scattering, amenable to both plasma conditions and to cold non-ionized targets, for which it was devised, was used. In the case of the partially ionized targets, the potential was approximated by the sum of two exponentially screened terms. The screening angle was calculated within the framework of the first Born approximation using the static screening approximation. In the Tables which give results for the fully ionized plasma the dynamically screened theory was employed (Lampe, 1970), the difference between both approximations is not significant as to the conclusions reached here. Clearly, the largest effect of scattering is attained by the lower energy electrons, the effect increasing with decreasing electron energy. In the examples cited here, the difference in scattering between cold and plasma targets is easily discernable for iron as well as for carbon using 2 MeV and 5 MeV electrons, in particular for the thicker target. However, even for the other beam energy combinations cited here, the difference in scattering should be observable, as well as for significantly less massive plasma columns.

ACKNOWLEDGEMENTS

This work was partially supported by the German Israeli Project Cooperation Foundation (DIP) and by the Israel Science Foundation.

REFERENCES

Barriga-Carrasco, M.D., Maynard, G. & Kurilenkov, Y. (2004). Influence of transverse diffusion within the proton beam fast-ignitor scenario. *Phys. Rev. E* **70**, 066407.

Barriga-Carrasco, M.D. & Potekhin, A.Y. (2006). Proton stopping in plasmas considering e(-)-e(-) collisions. *Laser Part. Beams* **24**, 553–558.

Bethe, H. (1953). Moliere's theory of multiple scattering. *Phys. Rev.* **89**, 1256.

Bichel, H. (1958), Multiple scattering of protons. *Phys Rev*. **111**, 182.

Bret, A., Firpo, M.C. & Deutsch, C. (2007). About the most unstable modes encountered in beam plasma interaction physics. *Laser Part. Beams* **25**, 117–119.

Deutsch, C., Furukawa, H., Mima, K., Murakami, M. & Nishihara, K. (1996). Interaction physics of the fast ignitor concept. *Phys. Rev. Lett*. **77**, 2483.

Fano, U. (1954). Inelastic collisions and the Moliere theory of multiple scattering. *Phys. Rev*. **93**, 117.

Firpo, M.C., Lifschitz, A.F., Lefebvre, E. & Deutsch, C. (2006). Early out of equilibrium beam-plasma evolution. *Phys. Rev. Lett.* **96**, 115004.

Flippo, K., Hegelich, B.M., Albright, B.J., Yin, L., Gautier, D.C., Letzring, S., Schollmeier, M., Schreiber, J., Schulze, R. & Fernandez, J.C. (2007). Laser-driven ion accelerators: Spectral control, monoenergetic ions and new acceleration mechanisms. *Laser Part. Beams* **25**, 3–8.

Glinec, Y., Faure, J., Pukhov, A., Kiselev, S., Gordienko, S., Mercier, B. & Malka, V. (2005). Generation of quasi-monoenergetic electron beams using ultrashort and ultraintense laser pulses. *Laser Part. Beams* **23**, 161–166.

Hanson, A.O., Lanzel, L.H., Lyman, E.M. & Scott, M.B. (1955). Measurement of Multiple Scattering of 15.7 MeV Electrons. *Phys. Rev*. **84**, 634.

Hoffmann, D.H.H., Weyrich, K., Wahl, H., Gardes, D., Bimbot, R. & Fleurier, C. (1990). Energy-loss of heavy-ions in a plasma target. *Phys. Rev. A* **42**, 2313–2321.

Jung, R., Osterholz, J., Lowenbrük, K., Kiselev, S., Pretzler, G., Pukhov, A., Willi, O., Kar, S., Borghesi, M., Nazarov, W., Karsch, S., Clarke, R. & Neely, D. (2005). Study of Electron-Beam Propagation through preionized dense foam plasma. *Phys. Rev. Lett*. **94**, 195001.

Koyama, K., Adachi, M., Miura, E., Kato, S., Masuda, S., Watanabe, T., Ogata, A. & Tanimoto, M. (2006). Monoenergetic electron beam generation from a laser-plasma accelerator. *Laser Part. Beams* **24**, 95–100.

Kulchitsky, L.A. & Latyshev, G.D. (1942). The multiple scattering of fast electrons. *Phys. Rev*. **61**, 254.

Lampe, M. (1970). Multiple scattering and energy loss of a fast test electron beam in a plasma. *Phys. Fluids* **13**, 2578.

Latter, R. (1955). Temperature behavior of the Thomas-Fermi statistical model for atoms. *Phys. Rev*. **99**, 1854.

Liberman, D. (1979). Self-consistent field model for condensed matter. *Phys. Rev*. **20**, 4981.

Lifschitz, A.F., Faure, J., Glinec, Y., Malka, V. & Mora, P. (2006). Proposed scheme for compact GeV laser plasma accelerator. *Laser Part. Beams* **24**, 255–259.

Mackinnon, A.J., Patel, P.K., Town, R.P., Edwards, M.J., Phillips, T., Lerner, S.C., Price, D.W., Hicks, D., Key, M.H., Hatchett, S., Wilks, S.C., Borghesi, M., Romagnani, L., Kar, S., Toncian, T., Pretzler, G., Willi, O., Koenig, M., Martinolli, E., Lepape, S., Benuzzi-Mounaix, A., Audebert, P., Gauthier, J.C., King, J., Snavely, R., Freeman, R.R. & Boehlly, T. (2004). Proton radiography as an electromagnetic field and density perturbation diagnostic. *Rev. Sci. Instrum*. **75**, 3531.

Moliere, G. (1947). Theorie der Streuung schneller gelandner Teilchen I, einzelstreuung am abgeschirmten Coulomb-Feld. *Naturforschg*. **2a**, 133.

Moliere, G. (1948). Theorie der Streuung schneller gelandner Teilchen II, mehrfach- und Vielfachstreuung. *Naturforschg*. **3a**, 78.

Nardi, E. & Zinamon, Z. (1978). Energy deposition by relativistic electrons in high-temperature targets. *Phys. Rev. A* **18**, 1246.

Nigam, B.P., Sundaresan, M.K. & Wu, T-Y. (1959). Theory of multiple scattering: second Born approximation and corrections to Moliere's work. *Phys. Rev*. **115**, 491.

Scott, W.T. (1963). The theory of small-angle multiple scattering of fast charged particles. *Rev. Mod. Phys*. **35**, 231.

Someya, T., Miyazawa, K., Kikuchi, T. & Kawata, S. (2006). Direct-indirect mixture implosion in heavy ion fusion. *Laser Part. Beams* **24**, 359–369.

Vincour, J. & Bem, P. (1978). Multiple scattering of fast charge particles in Silicon. *Nucl. Instr. and Meth. B* **148**, 399.

Wetzler, H., Suss, W., Stockl, C., Tauschwitz, A. & Hoffmann, D.H.H. (1997). Density diagnostics of an argon plasma by heavy ion beams and spectroscopy. *Laser Part. Beams* **15**, 449–459.

Yin, L., Albright, B.J., Hegelich, B.M. & Fernandez, J.C. (2006). GeV laser ion acceleration from ultrathin targets: The laser break-out afterburner. *Laser Part. Beams* **24**, 291–298.

https://doi.org/10.1017/S0263034607000602 Published online by Cambridge University Press